Available online at www.sciencedirect.com
SCIENCE DIRECT®
Journal of Solid State Chemistry 177 (2004) 3971–3976
JOURNAL OF SOLID STATE CHEMISTRY
www.elsevier.com/locate/jssc

Synthesis and crystal structures of the layered uranyl tellurites $A_2[(UO_2)_3(TeO_3)_2O_2]$ (A = K, Rb, Cs)

Jonathan D. Woodward, Philip M. Almond, Thomas E. Albrecht-Schmitt*

Department of Chemistry, Auburn University, 179 Chemistry Building, AL 36849, USA

Received 26 May 2004; received in revised form 25 June 2004; accepted 26 June 2004
Available online 7 October 2004

Abstract

The reactions of UO_3 and TeO_3 with KCl, RbCl, or CsCl at 800 °C for 5 d yield single crystals of $A_2[(UO_2)_3(TeO_3)_2O_2]$ (A = K (**1**), Rb (**2**), and Cs (**3**)). These compounds are isostructural with one another, and their structures consist of two-dimensional $^2_\infty[(UO_2)_3(TeO_3)_2O_2]^{2-}$ sheets arranged in a stair-like topology separated by alkali metal cations. These sheets are comprised of zigzagging uranium(VI) oxide chains bridged by corner-sharing trigonal pyramidal TeO_3^{2-} anions. The chains are composed of dimeric, edge-sharing, pentagonal bipyramidal UO_7 moieties joined by edge-sharing tetragonal bipyramidal UO_6 units. The lone-pair of electrons from the TeO_3 groups are oriented in opposite directions with respect to one another on each side of the sheets rendering each individual sheet non-polar. The alkali metal cations form contacts with nearby tellurite oxygen atoms as well as with oxygen atoms from the uranyl moieties. Crystallographic data (193 K, Mo$K\alpha$, $\lambda = 0.7107$ Å): **1**, triclinic, space group $P\bar{1}$, $a = 6.7985(5)$ Å, $b = 7.0123(5)$ Å, $c = 7.8965(6)$ Å, $\alpha = 101.852(1)°$, $\beta = 102.974(1)°$, $\gamma = 100.081(1)°$, $V = 349.25(4)$ Å^3, $Z = 2$, $R(F) = 2.70\%$ for 98 parameters and 1697 reflections with $I > 2\sigma(I)$; **2**, triclinic, space group $P\bar{1}$, $a = 7.0101(6)$ Å, $b = 7.0742(6)$ Å, $c = 8.0848(7)$ Å, $\alpha = 105.590(2)°$, $\beta = 101.760(2)°$, $\gamma = 99.456(2)°$, $V = 367.91(5)$ Å^3, $Z = 2$, $R(F) = 2.36\%$ for 98 parameters and 1817 reflections with $I > 2\sigma(I)$; **3**, triclinic, space group $P\bar{1}$, $a = 7.0007(5)$ Å, $b = 7.5195(6)$ Å, $c = 8.4327(6)$ Å, $\alpha = 109.301(1)°$, $\beta = 100.573(1)°$, $\gamma = 99.504(1)°$, $V = 399.49(5)$ Å^3, $Z = 2$, $R(F) = 2.61\%$ for 98 parameters and 1965 reflections with $I > 2\sigma(I)$.

Keywords: Uranyl tellurite; Layered uranyl compound; Uranium (VI) tellurite; Flux crystal growth

1. Introduction

The chemistry of actinides in high oxidation states has been the focal point of a myriad of research efforts owing to its rich structural chemistry as well as the key roles it plays in the fate of nuclear waste [1,2], mineralogy [3], and heterogeneous oxidation catalysis [4,5]. Under oxidizing conditions the chemistry of uranium is dominated by the formation of uranyl compounds that contain the classical, approximately linear UO_2^{2+} cation. This cation is strongly oxophilic and binds a host of oxoanions to form zero-, one-, two-, and three-dimensional structures. One of the more unusual systems that has been described in the literature is that of uranyl tellurites. This system was originally recognized from a handful of minerals that include cliffordite, $UO_2(Te_3O_7)$ [6], moctezumite, $PbUO_2(TeO_3)_2$ [7], and schmitterite, $UO_2(TeO_3)$ [8]. The application of hydrothermal syntheses to the uranyl tellurite system has results in the isolation of a diverse family represented by $Pb_2UO_2(TeO_3)_3$ [9], α-$Tl_2[(UO_2)(TeO_3)_2]$ [10], $Na_8[(UO_2)_6(TeO_3)_{10}]$ [10], $K[UO_2Te_2O_5(OH)]$ [11], $Tl_3(UO_2)_2[Te_2O_5(OH)](Te_2O_6)\cdot 2H_2O$ [11], β-$Tl_2[UO_2(TeO_3)_2]$ [11], and $Sr_3[UO_2(TeO_3)_2(TeO_3)_2]$ [11].

Uranyl tellurites are often structurally dissimilar to one another and exhibit considerable variation in their dimensionality and coordination environments of the U(VI) centers and in the Te(IV) oxoanions present. For

*Corresponding author. Fax: +1-334-844-6959.
E-mail address: albreth@auburn.edu (T.E. Albrecht-Schmitt).

0022-4596/$ - see front matter © 2004 Elsevier Inc. All rights reserved.
doi:10.1016/j.jssc.2004.06.054

example, $K[UO_2Te_2O_5(OH)]$, β-$Tl_2[UO_2(TeO_3)_2]$, and $Sr_3[UO_2(TeO_3)_2(TeO_3)_2]$ contain linear uranyl (UO_2^{2+}) moieties ligated by four equatorial oxygen atoms to create UO_6 tetragonal bipyramids [11]. However, $PbUO_2(TeO_3)_2$ [7], $UO_2(TeO_3)$ [8], $Pb_2UO_2(TeO_3)_3$ [9], α-$Tl_2[(UO_2)(TeO_3)_2]$ [10], $Na_8[(UO_2)_6(TeO_3)_{10}]$ [10], and $Tl_3(UO_2)_2[Te_2O_5(OH)](Te_2O_6)\cdot 2H_2O$ [11] all possess UO_7 pentagonal bipyramids, while $UO_2(Te_3O_7)$ [6] incorporates UO_8 hexagonal bipyramids. Similarly, the coordination environment around the Te(IV) centers in these compounds are diverse as well. $PbUO_2(TeO_3)_2$ [7], $Pb_2UO_2(TeO_3)_3$ [9], $Na_8[(UO_2)_6(TeO_3)_{10}]$ [10], β-$Tl_2[UO_2(TeO_3)_2]$ [11], and $Sr_3[UO_2(TeO_3)_2(TeO_3)_2]$ [11] all possess pyramidal tellurite, TeO_3^{2-}, anions. In contrast, $UO_2(TeO_3)$ [8], $K[UO_2Te_2O_5(OH)]$ [11], and $Tl_3(UO_2)_2[Te_2O_5(OH)](Te_2O_6)\cdot 2H_2O$ [11] contain one-dimensional chains of corner-sharing, square pyramidal TeO_4 units, while TeO_{4+1} moieties are found in $UO_2(Te_2O_7)$ [6]. The structure α-$Tl_2[(UO_2)(TeO_3)_2]$ is particularly interesting in that it contains both TeO_3^{2-} anions as well as the newly observed $Te_2O_6^{4-}$ anion [10].

The flexible coordination modes of the tellurite groups, coupled with the stereochemically active lone-pairs of electrons from Te(IV) centers, can dramatically affect the overall solid-state topology of uranyl compounds. However, the general tendency is for oxoanions of halogens and chalcogens with nonbonding electrons to either not affect the overall dimensionality of uranyl compounds or to reduce it from two-dimensional to one-dimensional, as demonstrated by approximately two dozen uranyl iodates and selenites [12–26]. While two-dimensional structures dominate hexavalent uranium chemistry, one- and three-dimensional structures are less common [3]. The predisposition of U(VI) compounds for adopting layered structures is a direct consequence of uranyl-containing polyhedra generally condensing perpendicular to the terminal, trans dioxo, $(O{=}U{=}O)^{2+}$ unit [3,27]. However, this trend is not always observed in uranyl tellurites. For example, $PbUO_2(TeO_3)_2$ [7], β-$Tl_2[UO_2(TeO_3)_2]$ [11], and $Sr_3[UO_2(TeO_3)_2(TeO_3)_2]$ [11] are one-dimensional, $UO_2(TeO_3)$ [8], α-$Tl_2[(UO_2)(TeO_3)_2]$ [10], and $Tl_3(UO_2)_2[Te_2O_5(OH)](Te_2O_6)\cdot 2H_2O$ [11] are two-dimensional, and $UO_2(Te_3O_7)$ [6], $Pb_2UO_2(TeO_3)_3$ [9], and $Na_8[(UO_2)_6(TeO_3)_{10}]$ [10] have three-dimensional network structures. Therefore, it is clear that there are structural features present in the uranyl tellurite system that allow for the formation of atypical structure types with dimensionalities both higher and lower than expected. The ability of Te(IV) to bind four or five oxo groups in its inner sphere, in addition to three, as observed in $UO_2(TeO_3)$ [8] and $UO_2(Te_3O_7)$ [6], does not account for the variable lattice dimensionality behavior of uranyl tellurites because $PbUO_2(TeO_3)_2$ [7] forms one-dimensional chains, and $Pb_2UO_2(TeO_3)_3$ [9] and $Na_8[(UO_2)_6(TeO_3)_{10}]$ [10] form three-dimensional open framework architectures yet all contain only TeO_3 units. This paper reports the synthesis and crystal structures of three new layered alkali metal uranyl tellurites, $K_2[(UO_2)_3(TeO_3)_2O_2]$ (**1**), $Rb_2[(UO_2)_3(TeO_3)_2O_2]$ (**2**), and $Cs_2[(UO_2)_3(TeO_3)_2O_2]$ (**3**).

2. Experimental

Syntheses. UO_3 (99.8%, Strem), TeO_3 (99.9%, Cerac), KCl (99.9%, Fisher), RbCl (99%, Alfa-Aesar), and CsCl (99.9%, Aldrich) were used as received. Semi-quantitative SEM/EDX analyses were performed using a JEOL 840/Link Isis instrument. Typical EDX analyses are within 5% of ratios determined from single crystal X-ray diffraction experiments. *Caution! While UO_3 contains depleted U, standard procedures for handling radioactive materials should be followed* [28].

$A_2[(UO_2)_3(TeO_3)_2O_2]$ (A = K (**1**), Rb (**2**), Cs (**3**)). The reactants UO_3 (160 mg, 0.558 mmol), TeO_3 (49 mg, 0.279 mmol), and KCl (42 mg, 0.558 mmol) for **1**, UO_3 (145 mg, 0.505 mmol), TeO_3 (44 mg, 0.253 mmol), and RbCl (61 mg, 0.505 mmol) for **2**, and UO_3 (132 mg, 0.461 mmol), TeO_3 (41 mg, 0.231 mmol), and CsCl (78 mg, 0.461 mmol) for **3**, were each loaded into fused silica tubes. The tubes were evacuated, sealed, placed within a ceramic retort, and heated within a tube furnace at 800 °C for 5 d. The heating rate was 5 °C/min and the cooling rate was 0.50 °C/min. Upon reaching room temperature, the tubes were then cooled with liquid nitrogen to condense any gases that might cause a buildup in pressure. The resultant mixture in the tubes consisted of yellow needles of **1**–**3** among alkali metal uranates. EDX analysis for $K_2[(UO_2)_3(TeO_3)_2O_2]$ (**1**), $Rb_2[(UO_2)_3(TeO_3)_2O_2]$ (**2**), and $Cs_2[(UO_2)_3(TeO_3)_2O_2]$ (**3**) provided an A/U/Te ratio of 2:3:2.

2.1. Crystallographic studies

Yellow needles of **1** ($0.018\times0.018\times0.175\,mm^3$), **2** ($0.014\times0.017\times0.028\,mm^3$), and **3** ($0.016\times0.022\times0.040\,mm^3$) suitable for single crystal X-ray diffraction experiments were selected using a stereomicroscope and mounted on thin glass fibers with epoxy. These mounted crystals were secured on goniometer heads, cooled to −80 °C with an Oxford Cryostat, and optically aligned on a Bruker SMART APEX CCD X-ray diffractometer using a digital camera. The same data collection process was used for each sample. A rotation photo was taken for each crystal, and a preliminary unit cell was determined from 3 sets of 30 frames with 10 s exposure times using SMART software. All intensity measurements were performed using a graphite monochromator utilizing Mo$K\alpha$ radiation ($\lambda = 0.71073$ Å) from a sealed tube with a monocapillary collimator. For all compounds, the intensities of reflections of a sphere were

Table 1
Crystallographic data for $K_2[(UO_2)_3(TeO_3)_2O_2]$ (**1**), $Rb_2[(UO_2)_3(TeO_3)_2O_2]$ (**2**), and $Cs_2[(UO_2)_3(TeO_3)_2O_2]$ (**3**)

Compound	K-1	Rb-2	Cs-3
Formula mass	1271.48	1364.22	1459.12
Crystal system	Triclinic	Triclinic	Triclinic
Color and habit	Yellow needle	Yellow needle	Yellow needle
Space group	$P\bar{1}$ (No. 2)	$P\bar{1}$ (No. 2)	$P\bar{1}$ (No. 2)
a (Å)	6.7989(5)	7.0101(6)	7.0007(5)
b (Å)	7.0123(5)	7.0742(6)	7.5195(6)
c (Å)	7.8965(6)	8.0848(7)	8.4327(6)
α (deg.)	101.8520(10)	105.5090(15)	109.3010(13)
β (deg.)	102.9740(10)	101.7600(15)	100.5730(14)
γ (deg.)	100.0810(10)	99.4560(15)	99.5040(14)
V (Å^3)	349.25(4)	367.91(5)	399.49(5)
Z	4	4	4
T (°C)	−80	−80	−80
λ (Å)	0.71073	0.71073	0.71073
ρ_{calcd} (g cm^{-3})	6.045	6.157	6.065
μ (Mo$K\alpha$, cm^{-1})	394.48	434.55	384.58
$R(F)$ for $F_o^2 > 2\sigma(F_o^2)$[a]	0.0270	0.0236	0.0261
$R_w(F_o^2)$[b]	0.0684	0.0575	0.0602

[a] $R(F) = \sum ||F_o| - |F_c|| / \sum |F_o|$.
[b] $R_w(F_o^2) = [\sum[w(F_o^2 - F_c^2)^2] / \sum wF_o^4]^{1/2}$.

Table 2
Atomic coordinates and equivalent isotropic displacement parameters for $K_2[(UO_2)_3(TeO_3)_2O_2]$ (**1**)

Atom	x	y	z	$U_{(eq)}$(Å^2)[a]
U(1)	0	0	0	0.022(1)
U(2)	0.1670(1)	−0.3999(1)	0.2358(1)	0.012(1)
Te(1)	0.3118(1)	0.1610(1)	0.4824(1)	0.012(1)
K(1)	0.6020(2)	0.2929(2)	0.1600(2)	0.023(1)
O(1)	0.1980(9)	−0.0425(7)	0.2682(7)	0.035(1)
O(2)	0.2525(9)	0.3468(9)	0.3555(8)	0.043(2)
O(3)	0.5905(7)	0.1997(7)	0.4823(6)	0.021(1)
O(4)	0.0114(8)	−0.3188(6)	−0.0230(6)	0.019(1)
O(5)	−0.0543(8)	−0.3989(8)	0.3258(7)	0.022(1)
O(6)	0.4022(8)	−0.3920(7)	0.1583(6)	0.016(1)
O(7)	−0.2335(8)	−0.0364(8)	0.0750(9)	0.029(1)

[a] $U_{(eq)}$ is defined as one-third of the trace of the orthogonalized U_{ij} tensor.

collected by a combination of 3 sets of exposures. Each set had a different ϕ angle for the crystal, and each exposure covered a range 0.3° in ω. A total of 1800 frames were collected with an exposure time per frame of 30 s for **1–3**.

For **1–3**, determination of integrated intensities and global cell refinement were performed with the Bruker SAINT (v. 6.02) software package using a narrow-frame integration algorithm. A face-indexed analytical absorption correction was initially applied using XPREP [29]. Individual shells of unmerged data were corrected analytically and exported in the same format. These files were subsequently treated with a semiempirical absorption correction by SADABS [30]. The program suite SHELXTL (v 5.1) was used for space group

Table 3
Atomic coordinates and equivalent isotropic displacement parameters for $Rb_2[(UO_2)_3(TeO_3)_2O_2]$ (**2**)

Atom	x	y	z	$U_{(eq)}$ (Å^2)[a]
U(1)	0	0	0	0.020(1)
U(2)	0.3976(1)	−0.1709(1)	−0.2338(1)	0.011(1)
Te(1)	−0.1605(1)	−0.3147(1)	−0.4790(1)	0.013(1)
Rb(1)	0.7060(1)	0.3869(1)	−0.1680(1)	0.025(1)
O(1)	0.0370(8)	−0.2126(9)	−0.2626(7)	0.034(1)
O(2)	−0.3544(9)	−0.2499(9)	−0.3649(9)	0.042(2)
O(3)	−0.2016(8)	−0.5850(7)	−0.4897(6)	0.022(1)
O(4)	0.3180(7)	−0.0144(8)	0.0254(6)	0.020(1)
O(5)	0.3801(8)	0.0343(7)	−0.3240(6)	0.022(1)
O(6)	0.3984(7)	−0.3915(7)	−0.1591(6)	0.020(1)
O(7)	0.0399(8)	0.2157(8)	−0.0800(9)	0.029(1)

[a] $U_{(eq)}$ is defined as one-third of the trace of the orthogonalized U_{ij} tensor.

Table 4
Atomic coordinates and equivalent isotropic displacement parameters for $Cs_2[(UO_2)_3(TeO_3)_2O_2]$ (**3**)

Atom	x	y	z	$U_{(eq)}$(Å^2)[a]
U(1)	0	0	0	0.015(1)
U(2)	0.3975(1)	−0.1774(1)	−0.2290(1)	0.011(1)
Te(1)	−0.1536(1)	−0.3180(1)	−0.4702(1)	0.013(1)
Cs(1)	0.7056(1)	0.3692(1)	−0.1800(1)	0.023(1)
O(1)	0.0340(7)	−0.2275(8)	−0.2563(7)	0.023(1)
O(2)	−0.3554(9)	−0.2482(9)	−0.3692(9)	0.040(2)
O(3)	−0.2070(8)	−0.5787(7)	−0.4991(7)	0.020(1)
O(4)	0.3183(7)	−0.0131(7)	0.0267(6)	0.016(1)
O(5)	0.3686(8)	0.0066(7)	−0.3178(7)	0.019(1)
O(6)	0.4053(8)	−0.3810(7)	−0.1596(7)	0.019(1)
O(7)	0.0437(8)	0.1933(8)	−0.0810(8)	0.024(1)

[a] $U_{(eq)}$ is defined as one-third of the trace of the orthogonalized U_{ij} tensor.

determination (XPREP), direct methods structure solution (XS), and least-squares refinement (XL) [29]. The final refinements included anisotropic displacement parameters for all atoms and a secondary extinction parameter. Crystallographic details are listed in Table 1, atomic coordinates and isotropic thermal parameters are provided in Tables 2–4, and selected bond lengths and angles are available in Table 5. Additional details can be found in Supporting Information.

3. Results and discussion

3.1. Syntheses

Crystalline products of the title compounds were synthesized by heating a stoichiometric mixture of alkali metal chloride salts, UO_3, and TeO_3 in evacuated, fused-silica ampoules or in open ceramic crucibles, although the reactions in ampoules afforded higher quality

Table 5
Selected bond distances (Å) and angles (deg) for $K_2[(UO_2)_3(TeO_3)_2O_2]$ (**1**), $Rb_2[(UO_2)_3(TeO_3)_2O_2]$ (**2**), and $Cs_2[(UO_2)_3(TeO_3)_2O_2]$ (**3**)

	K-1	Rb-2	Cs-3
Bond distances (Å)			
U(1)–O(1)	2.346(5)	2.341(5)	2.352(5)
U(1)–O(1)′	2.346(5)	2.341(5)	2.352(5)
U(1)–O(4)	2.222(4)	2.218(5)	2.220(5)
U(1)–O(4)′	2.222(4)	2.218(5)	2.220(5)
U(1)–O(7)	1.811(6)	1.813(5)	1.805(5)
U(1)–O(7)′	1.811(6)	1.813(5)	1.805(5)
U(2)–O(1)	2.433(5)	2.451(5)	2.467(5)
U(2)–O(2)′	2.278(5)	2.283(5)	2.304(5)
U(2)–O(3)′	2.429(5)	2.402(5)	2.385(5)
U(2)–O(4)	2.310(5)	2.317(5)	2.322(5)
U(2)–O(4)′	2.252(5)	2.263(5)	2.262(5)
U(2)–O(5)	1.803(5)	1.801(5)	1.800(5)
U(2)–O(6)	1.833(5)	1.818(5)	1.816(5)
Te(1)–O(1)	1.879(5)	1.873(5)	1.862(5)
Te(1)–O(2)	1.845(5)	1.844(5)	1.841(5)
Te(1)–O(3)	1.867(5)	1.862(5)	1.858(5)
Angles (deg)			
O(5)–U(1)–O(6)	176.41(19)	175.1(2)	173.8(2)
O(7)–U(2)–O(7)′	180.0	180.0	180.0
O(1)–Te(1)–O(2)	89.1(3)	90.8(3)	92.7(3)
O(1)–Te(1)–O(3)	98.7(2)	97.0(2)	96.5(2)
O(2)–Te(1)–O(3)	95.7(2)	97.7(2)	99.1(3)

crystals. The title compounds are identified as small, yellow, prismatic needles. Several alkali metal uranates are also produced in these reactions. At high temperatures, the *A*Cl salts (*A* = K, Rb, and Cs) act as fluxes as well as reactants and homogenize the reaction mixtures. Heating times varied from 1–6 days, temperatures from 650 to 850 °C, and a number of stoichiometries were employed, some favoring the relative amounts of UO_3, others favoring TeO_3. Above 650 °C, the reduction of Te^{6+} to Te^{4+} is significant, thus accounting for the formation of the tellurites. At lower temperatures, however, the starting materials did not react appreciably. In general, increasing the relative amount of TeO_3 with respect to the other reactants, the reaction time, and temperature encouraged the formation of **1**–**3**. Attempts to isolate single crystals of the analogous Na^+ and Tl^+ uranyl tellurites were unsuccessful; single crystals of schmitterite, $UO_2(TeO_3)$, were obtained instead.

3.2. Structures

The structures $A_2[(UO_2)_3(TeO_3)_2O_2]$ (*A* = K (**1**), Rb (**2**), and Cs(**3**)) consist of layered, two-dimensional $^2_\infty[(UO_2)_3(TeO_3)_2O_2]^{2-}$ sheets that extend along the *a*-axis. The sheets are comprised of zigzagging uranium (VI) oxide chains connected by corner-sharing, trigonal pyramidal TeO_3^{2-} ligands. The chains, extending along the *a*-axis, are composed of pentagonal bipyramidal

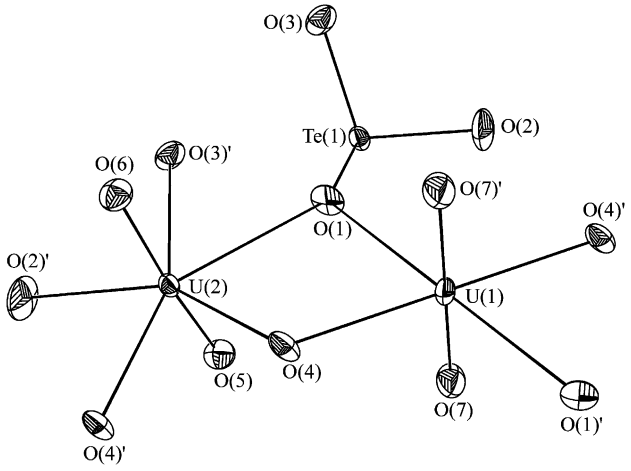

Fig. 1. A view of the fundamental building unit in $A_2[(UO_2)_3(TeO_3)_2O_2]$ (*A* = K (**1**), Rb (**2**), Cs (**3**)) consisting of pentagonal bipyramidal UO_7 and tetragonal bipyramidal UO_6 moieties and trigonal pyramidal TeO_3 units. 50% probability ellipsoids are shown (**3**).

UO_7 and tetragonal bipyramidal UO_6 moieties. Each of the uranyl units is coordinated equatorially by oxygen atoms from TeO_3^{2-} anions and bridging oxo ligands. The UO_7 pentagonal bipyramids form edge-sharing dimers that are connected by edge-sharing UO_6 polyhedra. The bridging TeO_3^{2-} anions join the dimers of UO_7 units on adjacent chains and form two opposite corners of the distorted UO_6 octahedra. The coordination polyhedra of the uranium atoms are completed by μ_3-O^{2-} ligands that are shared by both the UO_7 dimers and the UO_6 tetragonal bipyramids. Each UO_6 and UO_7 polyhedra contains two U–O bonds with the μ_3-O^{2-} ligands. Two or three additional sites are occupied by the oxo atoms from the TeO_3^{2-} anions for the UO_6 or UO_7 groups, respectively. The chains of tellurite ligands have their stereochemically active lone-pair of electrons oriented in opposite directions with respect to one another on each side of the sheet, rendering the individual sheets nonpolar. The basic building unit **3**, depicting the coordination environment of the uranium and tellurium atoms, is given in Fig. 1. A polyhedral representation of a single two-dimensional $^2_\infty[(UO_2)_3(TeO_3)_2O_2]^{2-}$ sheet is shown in Fig. 2.

The uranyl U=O bond lengths in the tetragonal bipyramidal UO_6 units are 1.811(6) (×2), 1.813(5) (×2), and 1.805(5) (×2) Å in **1**, **2**, and **3**, respectively. These bond lengths are similar to those in the pentagonal bipyramidal UO_7 moieties, which have U=O bond lengths of 1.803(5) and 1.833(5) Å for **1**, 1.801(5) and 1.818(5) Å for **2**, and 1.800(5) and 1.816(5) Å for **3**. The equatorial bond lengths in the pentagonal bipyramidal UO_7 units show significant variations of the U–O distances, ranging from 2.252(5) to 2.433(5) Å in **1**, 2.263(5) to 2.451(5) Å in **2**, and

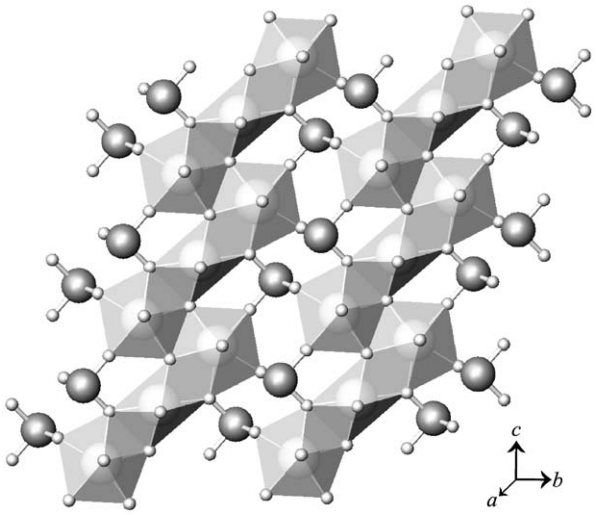

Fig. 2. An illustration of the $^{2}_{\infty}[(UO_2)_3(TeO_3)_2O_2]^{2-}$ sheets in $A_2[(UO_2)_3(TeO_3)_2O_2]$ (A = K (**1**), Rb (**2**), Cs (**3**)). The one-dimensional uranyl oxide zigzagging chains extending along the *a*-axis, shown in polyhedral form, consist of edge-sharing UO_7 pentagonal bipyramids and tetragonal bipyramidal UO_6 moieties. The chains are in turn linked by trigonal pyramidal TeO_3 units, shown in ball-and-stick form, into sheets.

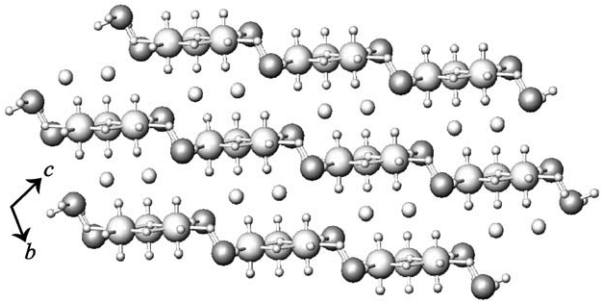

Fig. 3. A depiction of the structure of $A_2[(UO_2)_3(TeO_3)_2O_2]$ (A = K (**1**), Rb (**2**), Cs (**3**)) viewed perpendicular to the two-dimensional sheets down the *a*-axis showing the location of the interlayer alkali metal cations. The Te atoms are the smaller, darker shaded spheres and the U atoms are the larger, lighter shaded spheres within the sheets.

2.262(5) to 2.467(5) Å in **3**. The UO_6 groups are also distorted with equatorial bond lengths of 2.222(4) Å ($\times 2$) and 2.346(5) Å ($\times 2$) for **1**, 2.218(5) Å ($\times 2$) and 2.341(5) Å ($\times 2$) for **2**, and 2.220(5) Å ($\times 2$) and 2.352(5) Å ($\times 2$) for **3**. These distortions are due to differences in the coordination of the TeO_3^{2-} anions to the uranyl units versus coordination by the μ_3-O^{2-} anions. The U–O bonds from the tellurite oxygen atoms represent the long equatorial bonds while the μ_3-O atoms produce the short U–O equatorial bonds.

The TeO_3^{2-} ligands deviate significantly from idealized C_{3v} symmetry, exhibiting Te–O bond length variations consistent with their bridging modes to the uranium centers. The shorter Te–O bonds are to the μ_2-O(2) and μ_2-O(3) atoms (1.845(5) and 1.867(5) Å for **1**, 1.844(5) and 1.862(5) Å for **2**, and 1.841(5) and 1.858(5) Å for **3**) while the longer Te–O bonds are to the μ_3-O(1) atoms (1.879(5) Å for **1**, 1.873(5) Å for **2**, and 1.862(5) Å for **3**). The Te–O bond lengths are similar to those found in other uranyl tellurites with TeO_3^{2-} anions [6–11]. Bond valence sum calculations provide values of 5.97, 5.95, and 3.75 for **1**, 5.98, 5.99, and 3.78 for **2**, and 6.00, 5.97, and 3.82 for **3** for U(1), U(2), and Te(1), respectively. These bond-valence sums support the compounds containing U(VI) and Te(IV) [31,32]. Parameters for six- and seven-coordinate U(VI) from Burns et al. were used in these calculations [27].

The A^+ (A = K, Rb, and Cs) cations are found between the $^{2}_{\infty}[(UO_2)_3(TeO_3)_2O_2]^{2-}$ sheets. The cations interact with oxygen atoms from the UO_2^{2+} cations and the TeO_3^{2-} anions between adjacent sheets. Depending on where one establishes the maximum length for $A^+\cdots O$ contacts, there are approximately seven interactions with $A^+\cdots O$ distances ranging from 2.738(5) to 3.050(5) Å in **1**, 2.854(5) to 3.140(5) Å in **2**, and 2.998(5) to 3.262 Å in **3**. The shortest interactions between the Te(IV) centers and the alkali metal cations are 3.7167(5), 3.8475(8), and 4.0518(7) Å for **1**, **2**, and **3,** respectively. These distances are similar to those found in $K[UO_2Te_2O_5(OH)]$ (11). Based on these long distances, there is no evidence for interactions between the lone-pair of electrons and the alkali metal cations. In fact, the lone-pairs are not directed toward these cations. A view depicting the packing in **3**, perpendicular to the crystallographic *a*-axis, is shown in Fig. 3. The Te atoms are not coplanar with the adjacent U atoms that comprise the uranyl oxide one-dimensional chains thus giving rise to the stair-like topology of the sheets.

The structural topologies of the title compounds bear close resemblance to the $A_2[(UO_2)_3(IO_3)_4O_2]$ (A = K, Rb, and Tl) structure [14,16]. Both structures incorporate the zigzagging uranium oxide chains composed of edge-sharing UO_7 dimers connected by the edge-sharing UO_6 octahedra. However, while the tellurite ligands bridge the uranyl oxide chains to form two-dimensional sheets in the title compounds, while in $A_2[(UO_2)_3(IO_3)_4O_2]$ (A = K, Rb, and Tl), some of the iodate ligands coordinated to the uranyl oxide chains are terminal giving rise to a one-dimensional structure [14,16].

Comparing the title compounds with $UO_2(TeO_3)$, incorporation of the alkali metal cations has a dramatic affect on the resulting crystal structure. The sheets of schmitterite are comprised of linear chains of edge-sharing pentagonal bipyramidal UO_7 moieties bridged by corner sharing TeO_4 tetrahedra [8]. Furthermore, although both compounds have layered structures, schmitterite adopts a corrugated topology in contrast to the stair-like arrangement of the sheets within the title compounds [8].

4. Conclusions

This work demonstrates that molten salt reactions can be used to produce novel two-dimensional alkali metal uranyl tellurites $A_2[(UO_2)_3(TeO_3)_2O_2]$ (A = K (**1**), Rb (**2**), and Cs(**3**)). These compounds are dramatically different from uranyl tellurites synthesized using hydrothermal conditions. The structures of the title compounds consist of layered, two-dimensional sheets separated by alkali metal cations. The sheets are comprised of zigzagging uranium oxide chains containing both pentagonal bipyramidal UO_7 and tetragonal bipyramidal UO_6 moieties bridged by corner-sharing trigonal pyramidal TeO_3^{2-} anions. The title compounds not only further enhance the poorly represented area of uranyl tellurite chemistry, but demonstrate the flexibility of the TeO_3^{2-} ligand in producing new structures with diverse structural topologies.

Acknowledgment

This work was supported by the US Department of Energy, Office of Basic Energy Sciences, Heavy Elements Program (Grant DE-FG02-01ER15187).

Auxiliary Material: Further details of the crystal structure investigation may be obtained from the Fachinformationzentrum Karlsruhe, D-76344 Eggenstein-Leopoldshafen, Germany (Fax: (+49)7247-808-666; Email: crysdata@fiz-karlsruhe.de) on quoting depository numbers CSD 414064, 414063, and 414062.

References

[1] P.A. Finn, J.C. Hoh, S.F. Wolf, S.A. Slater, J.K. Bates, Radiochim. Acta 74 (1996) 65.
[2] K.-A. Hughes Kubatko, K.B. Helean, A. Navrotsky, P.C. Burns, Science 302 (2003) 1191.
[3] (a) P.C. Burns, M.L. Miller, R.C. Ewing, Can. Mineral. 34 (1996) 845
(b) P.C. Burns, Uranium: Mineralogy, Geochemistry and the Environment, in: P.C. Burns, R. Finch (Eds.), Mineralogical Society of America, Washington, DC, 1999 (Chapter 1);
(c) P.C. Burns, Mater. Res. Soc. Symp. Proc. 802 (2004) 89.
[4] H. Collette, V. Deremince-Mathieu, Z. Gabelica, J.B. Nagy, E.G. Derouane, J.J. Verbist, J. Chem. Soc. Faraday Trans 283 (1987) 1263.
[5] (a) G.C. Hutchings, C.S. Heneghan, I.D. Hudson, S.H. Taylor, Nature 384 (1996) 341;
(b) S.H. Taylor, C.S. Heneghan, G.J. Hutchings, I.D. Hudson, Catal. Today 59 (2000) 249;
(c) S.H. Taylor, G.J. Hutchings, M.-L. Palacios, D.F. Lee, Catal. Today 81 (2003) 171.
[6] (a) J. Galy, G. Meunier, Acta Crystallogr. B 27 (1971) 608;
(b) F. Branstätter, Tschermaks Mineral. Petrogr. Mitt. 29 (1981) 1.
[7] G.H. Swihart, P.K.S. Gupta, E.O. Schlemper, M.E. Back, R.V. Gaines, Am. Mineral. 78 (1993) 835.
[8] G. Meunier, J. Galy, Acta Crystallogr. B 29 (1973) 1251.
[9] F. Branstätter, Z. Kristallogr. 155 (1981) 193.
[10] P.M. Almond, M.L. McKee, T.E. Albrecht-Schmitt, Angew. Chem. Int. Ed. 41 (2002) 3426.
[11] P.M. Almond, T.E. Albrecht-Schmitt, Inorg. Chem. 41 (2002) 5495.
[12] R.E. Sykora, D.M. Wells, T.E. Albrecht-Schmitt, Inorg. Chem. 41 (2001) 2304.
[13] A.C. Bean, S.M. Peper, T.E. Albrecht-Schmitt, Chem. Mater. 13 (2001) 1266.
[14] A.C. Bean, M. Ruf, T.E. Albrecht-Schmitt, Inorg. Chem. 40 (2001) 3959.
[15] A.C. Bean, C.F. Campana, O. Kwon, T.E. Albrecht-Schmitt, J. Am. Chem. Soc. 123 (2001) 8806.
[16] A.C. Bean, T.E. Albrecht-Schmitt, J. Solid State Chem. 161 (2001) 416.
[17] P.M. Almond, S.M. Peper, E. Bakker, T.E. Albrecht-Schmitt, J. Solid State Chem. 168 (2002) 358.
[18] P.M. Almond, T.E. Albrecht-Schmitt, Inorg. Chem. 41 (2002) 1177.
[19] B.O. Loopstra, N.P. Brandenburg, Acta Crystallogr. B 34 (1978) 1335.
[20] V.E. Mistryukov, Y.N. Michailov, Koord. Khim. 9 (1983) 97.
[21] D. Ginderow, F. Cesbron, Acta Crystallogr. C 39 (1983) 824.
[22] D. Ginderow, F. Cesbron, Acta Crystallogr. C 39 (1983) 1605.
[23] M. Koskenlinna, J. Valkonen, Acta Crystallogr. C 52 (1996) 1857.
[24] M. Koskenlinna, I. Mutikainen, T. Leskelae, M. Leskela, Acta Chem. Scand. 51 (1997) 264.
[25] M.A. Cooper, F.C. Hawthorne, Can. Mineral. 33 (1995) 1103.
[26] M.A. Cooper, F.C. Hawthorne, Can. Mineral. 39 (2001) 797.
[27] P.C. Burns, R.C. Ewing, F.C. Hawthorne, Can. Mineral. 35 (1997) 1551.
[28] In our laboratory, uranium starting materials are stored in a glovebox or vented drawer until needed. All manipulations are carried out while we are wearing gloves and eye protection. All products are stored in a fume hood solely designated for radioactive materials.
[29 G.M. Sheldrick, SHELLXTL PC, Version 6.12, An Integrated System for Solving, Refining, and Displaying Crystal Structures from Diffraction Data; Siemens Analytical X-ray Instruments, Inc., Madison, WI, 2001.
[30] G.M. Sheldrick, SADABS 2001, Program for absorption correction using SMART CCD based on the method of Blessing: R.H. Blessing, Acta Crystallogr. A 1 (1995) 33.
[31] I.D. Brown, D. Altermatt, Acta Crystallogr. B 41 (1985) 244.
[32] N.E. Brese, M. O'Keeffe, Acta Crystallogr. B 47 (1991) 192.